Rebound Dynamics in Illusory Contrast-Driven Motion Perception

Hadar Cohen-Duwek (hadarco@openu.ac.il)
Elishai Ezra Tsur (elishai@nbel-lab.com)

Neuro-Biomorphic Engineering Lab (NBEL), Department of Mathematics and Computer Science
The Open University of Israel, Ra'anana, Israel

Abstract

Motion perception is a fundamental component of biological vision, and contrast-driven motion illusions offer a particularly revealing window into its underlying mechanisms. These phenomena include reverse-phi motion, in which contrast polarity inversion leads to the perception of motion opposite to the physical displacement, and Mario-type apparent motion, where coherent motion is perceived in the complete absence of spatial displacement. Existing computational accounts often rely on explicit interactions between contrast pathways, yet provide limited insight into the temporal structure of such percepts. Here, we propose a computational model in which rebound-driven temporal dynamics play a central role in generating illusory motion. The model reproduces the characteristic non-monotonic dependence of perceived motion direction on temporal offset observed in psychophysical data. Our results suggest that contrast-driven motion illusions can arise from timing-dependent perceptual dynamics rather than explicit pathway coupling, highlighting the importance of temporal computation in motion perception. The code is available at: https://github.com/NBELab/Cogsci2026

Keywords: motion perception; illusory motion; reverse-phi motion; apparent motion

Introduction

Motion perception is a fundamental component of biological vision, enabling organisms to infer object movement, self-motion, and environmental structure from dynamic visual input (Nakayama, 1985). Across species, motion signals support a wide range of perceptual and behavioral functions, including navigation and action planning, and are implemented by relatively simple neural circuits that extract spatiotemporal correlations from visual signals (Borst and Helmstaedter, 2015). This combination of behavioral relevance and circuit-level simplicity has made motion perception a central case study for linking neural dynamics to perceptual experience.

A prominent class of models describing early motion processing is correlation-based Elementary Motion Detectors (EMDs), originally proposed by Hassenstein and Reichardt (1953) to explain insect motion vision. Variants of this model have been shown to generalize across species, suggesting that correlation-based mechanisms reflect a fundamental computational principle rather than a species-specific solution (Borst and Groschner, 2023; Borst and Helmstaedter, 2015). At the same time, human and animal motion perception exhibits a range of visual illusions that place strong constraints on candidate computational models (Cohen-Duwek and Tsur, 2022; Cohen-Duwek et al., 2022).

One such illusion is reverse-phi motion, in which a stimulus physically displaced in one direction is perceived as moving in the opposite direction when contrast polarity is inverted between successive frames (Anstis, 1970), Figure 1A. Psychophysical studies have demonstrated that reverse-phi is not a simple inversion effect, but depends systematically on temporal parameters such as stimulus onset asynchrony, often showing non-monotonic timing dependence (Rogers et al., 2019; Wehrhahn, 2006). Importantly, reverse-phi effects have been observed not only in humans but also in insects, indicating that the underlying mechanisms arise early in the visual processing hierarchy and do not depend on cortical motion representations (Tuthill et al., 2011).

Cortical motion processing has often been described using motion energy models, which compute direction-selective responses through spatiotemporal filtering followed by energy normalization (Adelson and Bergen, 1985). While motion energy models successfully account for a wide range of motion phenomena in human vision, they abstract away from the ON and OFF pathway structure and transient nonlinear dynamics that characterize early visual circuits. As a result, they offer limited insight into how timing-dependent contrast-driven illusions such as reverse-phi might arise from biologically grounded neural mechanisms.

Other illusions related to reverse-phi include Mario-type apparent motion displays, in which observers perceive coherent motion despite the absence of any physical spatial displacement (Figure 1B). In these stimuli, motion is induced solely by temporal changes in contrast or luminance and can be viewed as a limiting case of reverse-phi motion with zero displacement i.e., $\Delta x = 0$ (Anstis, 1970; Rogers et al., 2019). While such displays can be predicted by using motion energy models (e.g., Johnson, 2023), they further emphasize the role of temporal asymmetries over spatial translation in driving motion perception.

Previous work (Cohen-Duwek and Spitzer, 2020) has suggested that reverse-phi motion may arise from rebound-like responses (Enroth-Cugell and Jones, 1963) following contrast offsets, without requiring explicit coupling between ON and OFF pathways. While this proposal identified rebound dynamics as a plausible computational principle, it remained abstract and did not provide a neural-level implementation or a systematic account of timing-dependent perceptual effects. As a result, it remains an open question whether reverse-phi

In G. Boleda, I. Dautriche, M. Maldonado, C. Saldana and T. Torrent (Eds.), *Proceedings of the 48th Annual Conference of the Cognitive Science Society*

motion fundamentally requires explicit ON/OFF interactions, or whether it can instead emerge from temporal nonlinearities operating within largely segregated contrast pathways (Adelson and Bergen, 1985; Borst and Helmstaedter, 2015).

In this work, we address these open questions by proposing a computationally explicit, biologically grounded extension of correlation-based motion detection that emphasizes rebound-driven temporal dynamics as a key explanatory principle. We suggest that incorporating such temporal asymmetries enables a single model to account for both the characteristic timing dependence of reverse-phi motion and Mario-type apparent motion displays, in which no physical displacement is present. By linking simple temporal computations to complex perceptual outcomes, the model offers a unified account of contrast-driven motion illusions and clarifies the computational principles underlying biological motion perception.

Methods

We implemented two closely matched computational models of motion detection to examine the role of rebound-driven temporal dynamics in contrast-based motion perception. Both models share the same overall architecture and stimulus timing, but differ in two key respects: the presence or absence of rebound-like temporal transients, and the manner in which ON and OFF polarity signals are combined. In the rebound-based model, ON and OFF pathways remain uncoupled and interact only through timing-dependent dynamics within each pathway. In contrast, the non-rebound model follows the classical formulation of EMD in which polarity information is explicitly mixed within the motion computation. This design, Figure 1E, allows a direct comparison between model variants while controlling for all other factors.

Neuronal implementation

Units are modeled as LIFRate neurons producing continuous activity traces (Gerstner et al., 2014). Direction selectivity emerges from delayed coincidence detection at the network level. Rebound is implemented as a presynaptic temporal transformation of the input current and is absent in the control model.

Rebound mechanism

Post-inhibitory rebound refers to a transient increase in activity that occurs following the release from inhibition, reflecting a temporal asymmetry between inhibitory suppression and subsequent recovery (Spitzer et al., 1993). In the present formulation, rebound is treated as a functional computational mechanism rather than a specific biophysical process, capturing the delayed excitatory transient that follows contrast offset or polarity reversal.

Post-inhibitory rebound dynamics were modeled using a set of coupled first-order differential equations that capture the interaction between fast and slow inhibitory components and their subsequent release, Figure 1C.

Formally, let $u(t)$ denote the effective input to the circuit. The input is first decomposed into rectified excitatory and inhibitory components:

$$\begin{aligned} \mathrm{exc}(t) &= \max(u(t), 0), \\ \mathrm{inh}(t) &= \max(-u(t), 0). \end{aligned} \tag{1}$$

These definitions reflect the unidirectional nature of excitatory and inhibitory (GABAergic) synaptic inputs via half-wave rectification. The inhibitory drive is then processed by two low-pass synaptic filters with distinct time constants:

$$\begin{aligned} \tau_{\mathrm{inh}} \frac{dx_1(t)}{dt} &= -x_1(t) + \mathrm{inh}(t), \\ \tau_{\mathrm{delay}} \frac{dx_2(t)}{dt} &= -x_2(t) + x_1(t) \end{aligned} \tag{2}$$

where $x_1(t)$ models fast inhibition (e.g., GABA_A) and $x_2(t)$ models a slower inhibitory or intrinsic component, e.g., GABA_B or recovery of T-type Ca^{2+} channels, (Nicoll, 2004). Post-inhibitory release is generated by the difference between the slow and fast pathways:

$$\begin{aligned} r_{\mathrm{diff}}(t) &= x_2(t) - x_1(t), \\ r(t) &= \max\big(r_{\mathrm{diff}}(t), 0\big). \end{aligned} \tag{3}$$

where $r_{\mathrm{diff}}(t)$ denotes the unrectified difference between the slow and fast inhibitory pathways, representing the initial release signal before thresholding. The rectified release signal is then integrated through a low-pass filter:

$$\tau_{\mathrm{reb}} \frac{dx_3(t)}{dt} = -x_3(t) + k_{\mathrm{reb}}\, r(t), \tag{4}$$

where $x_3(t)$ represents the integrated rebound depolarization, modeling the membrane-level accumulation of inward currents that generate post-inhibitory rebound firing. The final current injected into the target neuron that combines instantaneous excitation rebound depolarization, and the hyperpolarizing inhibitory penalty:

$$I_{\mathrm{neuron}}(t) = \mathrm{exc}(t) + x_3(t) - k_{\mathrm{inh}}\, \mathrm{inh}(t), \tag{5}$$

Although simplified, this formulation captures key biophysical features of post-inhibitory rebound: a transient depolarization following inhibition, asymmetric temporal filtering, and dependence on the duration and amplitude of preceding inhibitory input.

Figure 1D illustrates the rebound mechanism in ON and OFF neurons. During a positive stimulus, the OFF neuron is suppressed and exhibits a transient rebound response upon stimulus offset; analogously, the ON neuron shows a rebound response following termination of a negative stimulus.

Model architectures

To isolate the contribution of the rebound mechanism, we implemented a control model that removes all presynaptic rebound dynamics and relies on standard LIFRate neurons, Figure 1D. This variant corresponds to a classical Elementary

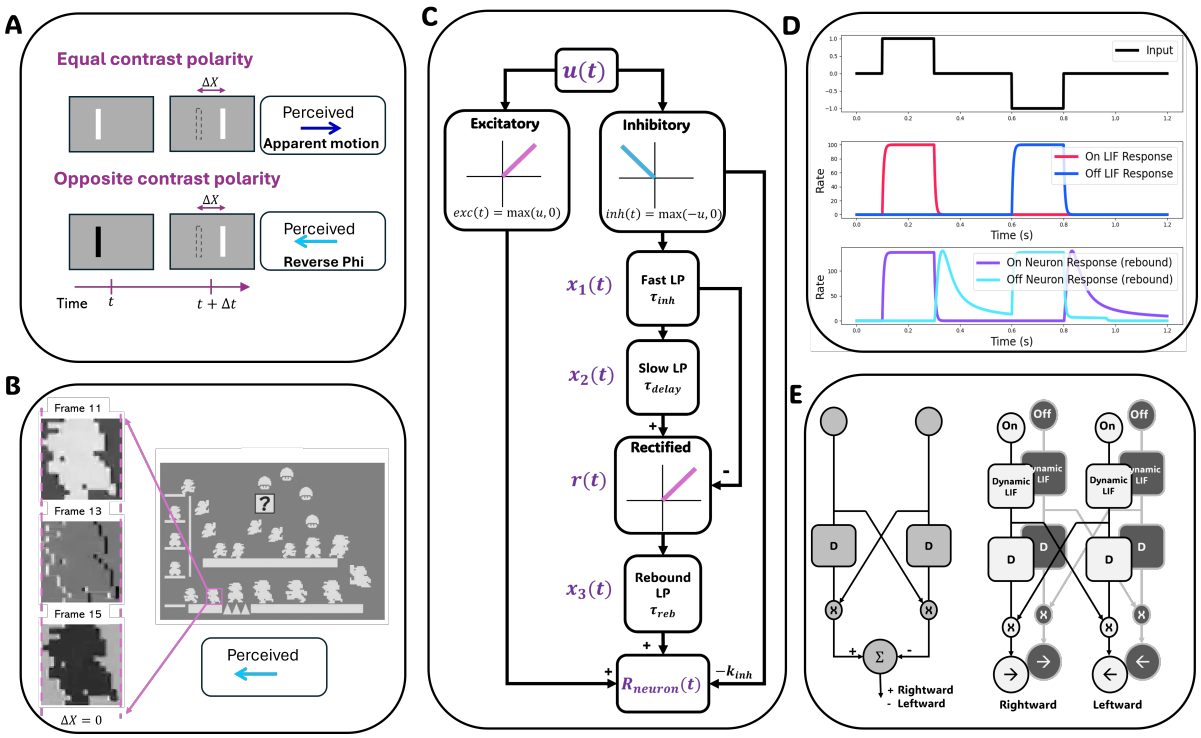

Figure 1: Schematic illustration of rebound-based motion detection and related motion phenomena. (A) Apparent motion with preserved versus inverted contrast polarity, yielding physical-direction motion and reverse-phi motion, respectively. (B) Mario-type apparent motion: a static image sequence ($\Delta x = 0$) perceived as motion due solely to temporal contrast changes; the highlighted object is perceived as moving leftward. (C) Conceptual flow of the rebound computation from input $u(t)$ through intermediate states to a transient rebound response $r(t)$. (D) Example neural responses to an ON/OFF stimulus: standard neurons show sustained activity, whereas rebound-enabled neurons exhibit transient post-inhibitory responses. (E) Direction-selective motion models: a coupled non-rebound model (left) and an uncoupled rebound-based model (right).

Motion Detector (EMD), in which motion selectivity arises from delayed coincidence detection and ON and OFF pathways are allowed to mix at the correlation stage, rather than being maintained as separate functional channels, (Hassenstein and Reichardt, 1953).

Both models implement a delay-and-multiply motion detection scheme operating on two spatially separated input signals. The models differ in whether transient responses are generated by an explicit rebound mechanism and in whether ON and OFF polarity channels are preserved as independent computational streams or allowed to mix during correlation.

Rebound-based, polarity-separated (uncoupled) EMD model The first model implements a polarity-specific motion detector in which ON and OFF channels are maintained as separate functional pathways throughout the computation. Let $x_L(t)$ and $x_R(t)$ denote the left and right input signals. These inputs are decomposed into ON and OFF components.

$$\begin{aligned} x_{\mathrm{ON}}(t) &= \max(x(t), 0), \\ x_{\mathrm{OFF}}(t) &= \max(-x(t), 0). \end{aligned} \tag{6}$$

This yields four signals $x_{L,\mathrm{ON}}, x_{L,\mathrm{OFF}}, x_{R,\mathrm{ON}}, x_{R,\mathrm{OFF}}$. Each polarity channel is passed through a rebound-generating stage that produces transient activity at stimulus transitions. The resulting rebound-shaped signals are denoted

$$y_{L,\mathrm{ON}}(t),\ y_{L,\mathrm{OFF}}(t),\ y_{R,\mathrm{ON}}(t),\ y_{R,\mathrm{OFF}}(t).$$

(For a full mathematical description of the rebound dynamics, see the section above.)

Direction selectivity is computed using a classical delay-and-multiply scheme applied independently to the ON and OFF pathways. For the ON channels, the rightward and leftward motion energies are given by

$$\begin{aligned} C_{\rightarrow,\mathrm{ON}}(t) &= y^d_{L,\mathrm{ON}}(t)\, y_{R,\mathrm{ON}}(t), \\ C_{\leftarrow,\mathrm{ON}}(t) &= y^d_{R,\mathrm{ON}}(t)\, y_{L,\mathrm{ON}}(t), \end{aligned} \tag{7}$$

with an analogous computation for the OFF channels:

$$\begin{aligned} C_{\rightarrow,\mathrm{OFF}}(t) &= y^d_{L,\mathrm{OFF}}(t)\, y_{R,\mathrm{OFF}}(t), \\ C_{\leftarrow,\mathrm{OFF}}(t) &= y^d_{R,\mathrm{OFF}}(t)\, y_{L,\mathrm{OFF}}(t). \end{aligned} \tag{8}$$

Here, the superscript d indicates a temporally delayed signal. The final motion signal is obtained by subtracting leftward from rightward energy across both polarities,

$$M_{\mathrm{rebound}}(t) = \left(C_{\rightarrow,\mathrm{ON}} + C_{\rightarrow,\mathrm{OFF}}\right) - \left(C_{\leftarrow,\mathrm{ON}} + C_{\leftarrow,\mathrm{OFF}}\right), \tag{9}$$

yielding a signed estimate of motion direction and strength.

Non-rebound, polarity-mixed (coupled, classical EMD) model The second model serves as a control and corresponds to a classical Elementary Motion Detector (EMD). In this variant, transient responses arise solely from standard leaky integrate-and-fire dynamics and explicit temporal delays, without any rebound mechanism. Moreover, ON and OFF channels are not treated as independent streams but are allowed to interact directly during the correlation stage.

As above, the left and right inputs are decomposed into polarity components. Delayed left-channel activity is multiplied with instantaneous right-channel activity, allowing both same-polarity and mixed-polarity interactions:

$$\begin{aligned} C^+(t) &= y^d_{L,\mathrm{ON}}(t)\, y_{R,\mathrm{ON}}(t) + y^d_{L,\mathrm{OFF}}(t)\, y_{R,\mathrm{OFF}}(t), \\ C^-(t) &= y^d_{L,\mathrm{ON}}(t)\, y_{R,\mathrm{OFF}}(t) + y^d_{L,\mathrm{OFF}}(t)\, y_{R,\mathrm{ON}}(t). \end{aligned} \tag{10}$$

The net motion signal is then computed as

$$M_{\mathrm{EMD}}(t) = C^+(t) - C^-(t), \tag{11}$$

which implements a polarity-mixed coincidence detector consistent with classical Reichardt-type formulations.

Computational implementation

The proposed motion models were implemented using the Neural Engineering Framework (NEF; Bekolay et al., 2014; Stewart and Eliasmith, 2014) as a general-purpose tool for instantiating dynamical systems in neural populations. NEF is used here strictly as an implementation framework; the core contributions of the model lie in the structure and temporal dynamics of the motion detectors rather than in the representational assumptions of the framework itself.

For reverse-phi motion, the model is evaluated at the level of a single motion detector receiving temporally offset inputs from two spatial locations. In contrast, Mario-type apparent motion is modeled using an array of local motion detectors that combine signals from neighboring pixels, followed by simple spatial pooling across adjacent detectors to yield coherent regional motion percepts.

Model parameters Unless otherwise stated, both models used identical stimulus timing and delay structure. Input pulses had a duration of $T_p = 5$–10 ms, and the inter-channel delay ΔT was varied parametrically. In the rebound-based model, rebound dynamics were governed by time constants $\tau_{\mathrm{inhib}} = 12$ ms, $\tau_{\mathrm{delay}} = 17$ ms, and $\tau_{\mathrm{rebound}} = 10$ ms, with inhibitory and rebound gains $k_{\mathrm{inhib}} = 12$ and $k_{\mathrm{rebound}} = 6$. Temporal delays in the correlation stage were implemented using synaptic filtering with an effective delay of approximately 50ms. All other parameters were held constant across models to enable a direct comparison.

Results

This section evaluates the ability of the proposed models to account for behavioral phenomena associated with contrast-driven motion perception. We first compare model predictions to psychophysical data from classical reverse-phi experiments, focusing on the dependence of perceived motion direction on temporal offset, Figure 2. We then examine whether the same computational principles generalize to Mario-type apparent motion displays, in which coherent motion is perceived despite the absence of any physical spatial displacement, Figure 3. Together, these analyses assess the extent to which the models capture both the directionality and temporal structure of contrast-driven motion illusions.

Comparison between model predictions and human observer data

Figure 2A, shows psychophysical measurements from three different experiments performed by Wehrhahn (2006), plotting perceived motion direction as a function of the temporal offset ΔT between successive frames in a reverse-phi stimulus. Across observers, perceived motion exhibits a clear non-monotonic dependence on ΔT, including direction inversion at short temporal offsets and a transition toward the opposite percept at longer delays. While the precise transition points vary across observers, the qualitative timing dependence is consistent.

To enable a direct comparison between model predictions and psychophysical findings reported by Wehrhahn (2006), behavioral performance curves in Figure 2A were first transformed into a binary motion-direction measure. Specifically, for each observer and temporal offset, perceived motion was classified as rightward $(+1)$ when the proportion of correct responses exceeded 0.5, and as leftward (-1) when performance fell below 0.5. This binarization extracts the dominant perceived motion direction and allows a direct qualitative comparison with the sign of the model's directional output.

Figure 2B shows the resulting perceived motion direction as a function of temporal offset for human observers, reproduced from Wehrhahn's reverse-phi experiment (Wehrhahn, 2006), alongside predictions of the two model variants. Consistent with the original psychophysical findings, human observers exhibit a non-monotonic dependence on temporal offset, with perceived motion reversing direction at short delays and transitioning back to the physical direction at longer offsets. The rebound-based (uncoupled) model closely reproduces this pattern, capturing both the direction inversion and the timing of the transition. In contrast, the non-rebound (coupled) model predicts a largely invariant motion direction across temporal offsets and fails to account for the timing-dependent reversal reported by Wehrhahn (2006). Together, these results suggest that rebound-driven temporal dynamics are necessary to reproduce the temporal structure of reverse-phi perception observed in psycho-physical data.

Model predictions for Mario-type apparent motion

To test whether the proposed models generalize beyond classical reverse-phi displays, we evaluated their predictions on

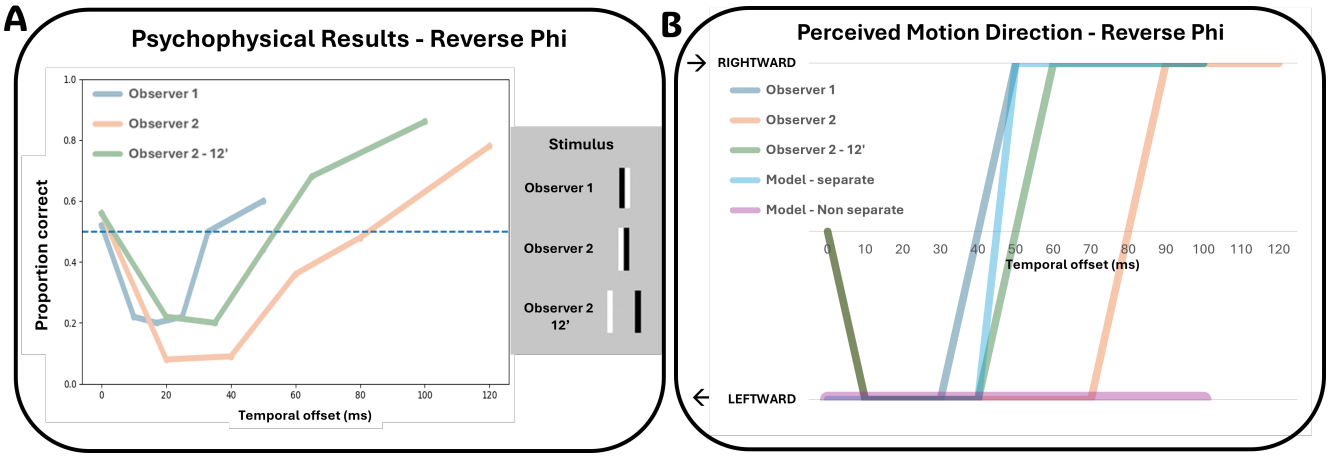

Figure 2: Behavioral data and model predictions for reverse-phi motion. (A) Perceived motion direction as a function of temporal offset ΔT in human observers, revealing a non-monotonic dependence on timing and direction inversion at short delays. Replotted based on data reported in Wehrhahn (2006). (B) Comparison between human data and model predictions. The rebound-based model reproduces both direction inversion and its systematic dependence on ΔT, whereas the non-rebound (classical EMD-like) model predicts a largely timing-invariant response.

Mario-type apparent motion stimuli, in which coherent motion is perceived despite the absence of any physical spatial displacement ($\Delta x = 0$). To this end, the motion detectors described above were extended beyond horizontal motion to include analogous detectors for vertical motion. From the original Mario display, four distinct objects were selected, each consistently perceived as moving in a different direction (downward, upward, leftward, and rightward).

Figure 3 demonstrates a clear qualitative difference between the two model variants. For example, in the upward apparent motion condition, the rebound-based model produces a stable and consistent motion signal in the expected direction, reflected by a predominance of upward-coded responses (yellow) across frames. In contrast, the non-coupled (non-rebound) model fails to converge on a single motion direction, yielding a mixture of responses corresponding to upward, leftward, and rightward motion. Similar patterns are observed across the other apparent motion directions, indicating that rebound-driven temporal dynamics are necessary for generating coherent directional percepts in the absence of physical displacement.

Discussion

The present study examined whether a single computational principle can account for multiple forms of contrast-driven motion perception. We compared two classes of correlation-based motion models, one incorporating rebound-driven temporal dynamics and one without, against psychophysical data on reverse phi motion and Mario-type apparent motion displays. Crucially, the rebound-based model operates without explicit coupling or mixing between ON and OFF pathways, unlike standard EMD formulations that assume polarity integration within the motion computation. Only the rebound-based model reproduces the characteristic timing dependence of reverse phi perception and generalizes to apparent motion without physical displacement, whereas the non-rebound model fails in both cases.

Together, these findings indicate that rebound-driven temporal dynamics offer a compact and unifying account of contrast-driven motion illusions. A single model captures both the timing-dependent reversal observed in reverse-phi motion and the coherent percepts elicited by Mario-type apparent motion without displacement. Importantly, the results suggest that such motion illusions arise as natural byproducts of rebound dynamics within otherwise segregated pathways; without rebound responses, these illusory percepts would not emerge.

A central empirical constraint on models of reverse-phi motion is the systematic dependence of perceived motion direction and strength on the inter-stimulus delay ΔT (Wehrhahn, 2006). Reverse-phi perception exhibits a non-monotonic temporal profile, placing strong demands on computational models to account for temporal asymmetries rather than relying on a fixed inversion rule. While both model variants produce direction inversion under classical conditions, only the rebound-based model captures the graded modulation of motion percepts across temporal offsets. In this model, the timing of the rebound response relative to the incoming sensory signal biases motion detectors toward an illusory direction, whereas the non-rebound EMD remains largely insensitive to ΔT.

This sensitivity to temporal structure extends beyond stimuli involving physical displacement. For Mario-type apparent motion displays, in which no spatial displacement is present ($\Delta x = 0$), the non-rebound model does not yield a stable motion signal, Figure 3. By contrast, the rebound-based model

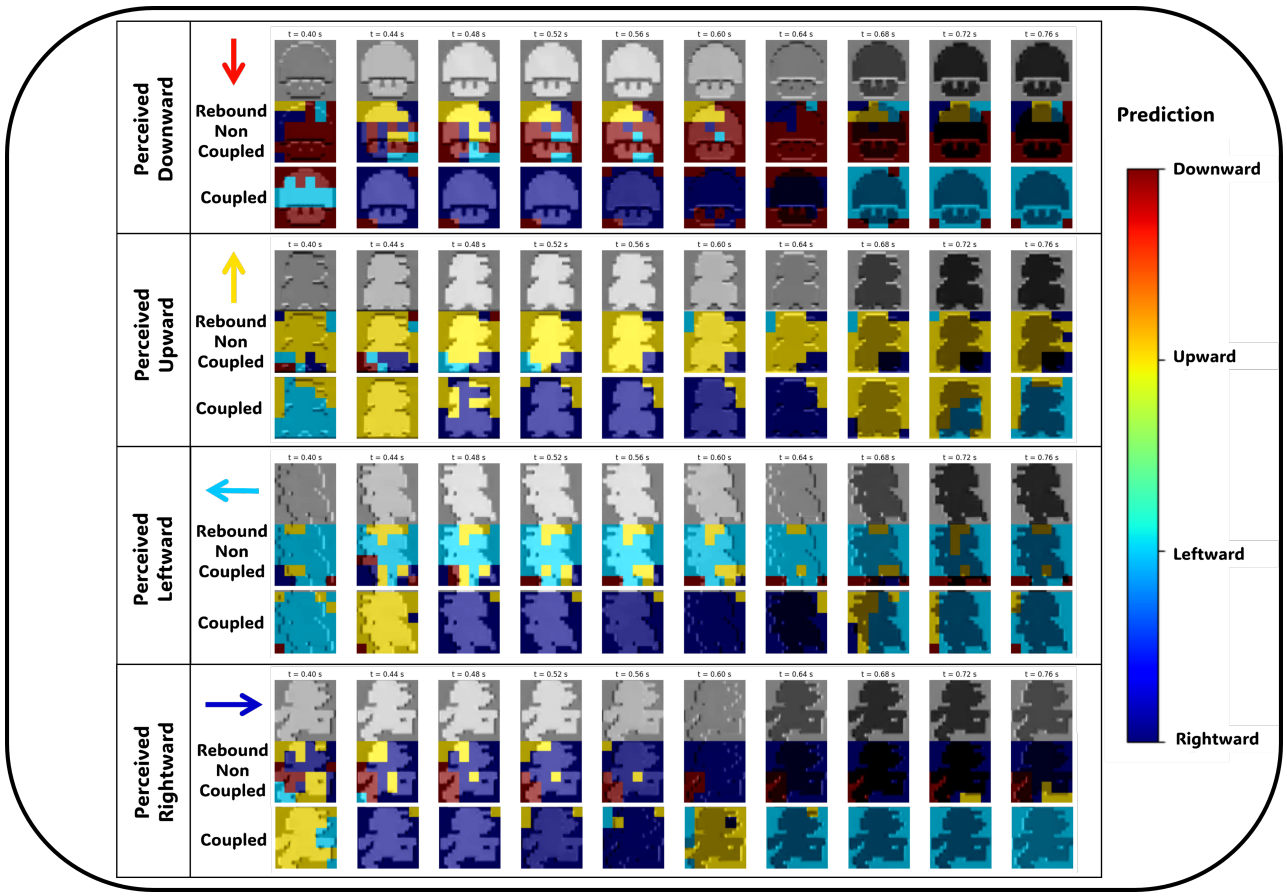

Figure 3: Model predictions for reverse-phi and Mario-type apparent motion. Stimulus sequences and corresponding model-derived motion signals for Mario-type displays ($\Delta x = 0$), organized into four apparent motion directions, each encoded by a distinct color. For each motion type, the top row shows the original stimulus sequence, the middle row shows predictions of the non-coupled (non-rebound) model, and the bottom row shows predictions of the coupled, rebound-based model.

predicts robust apparent motion whose direction and strength depend on temporal offset, supporting a unified computational account of contrast-driven motion phenomena rather than a special-purpose explanation for reverse-phi alone, Figure 3.

More broadly, these findings inform ongoing debates regarding the role of ON and OFF pathway interactions in motion perception. Whereas many classical models assume explicit polarity mixing, the present results suggest that timing-dependent motion percepts can arise without direct coupling between ON and OFF channels. From a computational perspective, apparent polarity integration at the perceptual level need not correspond to explicit signal mixing at the level of motion detection, but may instead emerge from asymmetric temporal dynamics operating within segregated contrast pathways. Motion-energy models characterize direction selectivity in terms of spatiotemporal phase relationships, but typically treat these relationships as descriptive primitives rather than deriving them from underlying neural dynamics, and are often framed at a cortical level, assuming relatively complex spatiotemporal filtering. In contrast, the present account shows how comparable temporal asymmetries can arise from simple rebound dynamics at the level of elementary neural units. This interpretation is consistent with physiological evidence for direction-selective responses arising from relatively simple antagonistic center-surround mechanisms in the mammalian retina (Ankri et al., 2020), suggesting that temporally asymmetric inhibition-release dynamics can support motion selectivity already at early stages of visual processing.

Finally, we note that the proposed model is restricted to temporal dynamics and does not incorporate spatial interactions or extended spatial context. As a result, it does not account for motion phenomena that critically depend on spatial structure, such as spatially complex reverse-motion effects (Wehrhahn, 2006). Extending the framework to include spatial interactions will be an important direction for future work, allowing assessment of how rebound-driven temporal mechanisms interact with spatial organization and other visual cues in shaping motion perception (Rogers et al., 2019).

Acknowledgments

The authors thank the members of the Neuro-Biomorphic Engineering Lab at the Open University of Israel and Hedva Spitzer (Tel Aviv University) for the insightful discussions.

References

Adelson, E. H., & Bergen, J. R. (1985). Spatiotemporal energy models for the perception of motion. *Journal of the optical society of america A*, *2*(2), 284–299.

Ankri, L., Ezra-Tsur, E., Maimon, S. R., Kaushansky, N., & Rivlin-Etzion, M. (2020). Antagonistic center-surround mechanisms for direction selectivity in the retina. *Cell reports*, *31*(5).

Anstis, S. (1970). Phi movement as a subtraction process. *Vision research*, *10*(12), 1411–IN5.

Bekolay, T., Bergstra, J., Hunsberger, E., DeWolf, T., Stewart, T. C., Rasmussen, D., Choo, X., Voelker, A. R., & Eliasmith, C. (2014). Nengo: A python tool for building large-scale functional brain models. *Frontiers in neuroinformatics*, *7*, 48.

Borst, A., & Groschner, L. N. (2023). How flies see motion. *Annual review of neuroscience*, *46*(1), 17–37.

Borst, A., & Helmstaedter, M. (2015). Common circuit design in fly and mammalian motion vision. *Nature neuroscience*, *18*(8), 1067–1076.

Cohen-Duwek, H., Slovin, H., & Ezra Tsur, E. (2022). Computational modeling of color perception with biologically plausible spiking neural networks. *PLoS Computational Biology*, *18*(10), e1010648.

Cohen-Duwek, H., & Spitzer, H. (2020). The rebound response plays a role in the motion mechanisms and perception. *bioRxiv*, 2019–12.

Cohen-Duwek, H., & Tsur, E. E. (2022). Biologically plausible illusionary contrast perception with spiking neural networks. *2022 IEEE International Conference on Image Processing (ICIP)*, 1586–1590.

Enroth-Cugell, C., & Jones, R. W. (1963). Responses of cat retinal ganglion cells to exponentially changing light intensities. *Journal of neurophysiology*, *26*(6), 894–907.

Gerstner, W., Kistler, W. M., Naud, R., & Paninski, L. (2014). *Neuronal dynamics: From single neurons to networks and models of cognition*. Cambridge University Press.

Hassenstein, B., & Reichardt, W. (1953). Der schluss von reiz-reaktions-funktionen auf system-strukturen. *Zeitschrift für Naturforschung B*, *8*(9), 518–524.

Johnson, J. (2023). *Motion illusions*. Retrieved December 14, 2025, from https://jake.vision/blog/motion-illusions

Nakayama, K. (1985). Biological image motion processing: A review. *Vision research*, *25*(5), 625–660.

Nicoll, R. A. (2004). My close encounter with gabab receptors. *Biochemical pharmacology*, *68*(8), 1667–1674.

Rogers, B., Anstis, S., Ashida, H., & Kitaoka, A. (2019). Reversed phi and the "phenomenal phenomena" revisited. *i-Perception*, *10*(4), 2041669519856906.

Spitzer, H., Almon, M., & Sandler, V. M. (1993). A model for detection of spatial and temporal edges by a single x cell. *Vision research*, *33*(13), 1871–1880.

Stewart, T. C., & Eliasmith, C. (2014). Large-scale synthesis of functional spiking neural circuits. *Proceedings of the IEEE*, *102*(5), 881–898.

Tuthill, J. C., Chiappe, M. E., & Reiser, M. B. (2011). Neural correlates of illusory motion perception in drosophila. *Proceedings of the National Academy of Sciences*, *108*(23), 9685–9690.

Wehrhahn, C. (2006). Reversed phi revisited. *Journal of Vision*, *6*(10), 2–2.